Science Advances

AAAS

advances.sciencemag.org/cgi/content/full/3/5/e1602055/DC1

Supplementary Materials for

Field-induced magnetic instability within a superconducting condensate

Daniel Gabriel Mazzone, Stéphane Raymond, Jorge Luis Gavilano, Eric Ressouche, Christof Niedermayer, Jonas Okkels Birk, Bachir Ouladdiaf, Gaël Bastien, Georg Knebel, Dai Aoki, Gérard Lapertot, Michel Kenzelmann

Published 19 May 2017, *Sci. Adv.* **3**, e1602055 (2017)
DOI: 10.1126/sciadv.1602055

This PDF file includes:

Supplementary Materials and Methods

Macroscopic results

For a substitution of 5% Nd the residual resistivity ratio (RRR) is about 3.6 (see fig. S1A and (*28*)). In $CeCoIn_5$ the optimization of the crystal synthesis increased the RRR from the first reported experimental realization, RRR ≈ 5.5 (*7*), up to values over 300 (*37*). The reduction of the RRR value in $Nd_{0.05}Ce_{0.95}CoIn_5$ compared to $CeCoIn_5$ provides evidence that small Nd concentrations act as a source of disorder.

Temperature dependent heat capacity results for magnetic fields applied in the basal plane are plotted in fig. S1B. The discontinuity in the thermal heat capacity that is assigned to the superconducting transition was used to determine part of the superconducting phase boundary (see fig. S1B inset). A slight increase in the heat capacity is observed in the paramagnetic state at lowest temperatures around T = 1 K and $\mu_0 H$ = 8 T. However, the temperature limitations (T > 600 mK) and the signature of the superconducting transition prevent the direct observation of quantum fluctuations by means of thermal heat capacity. In these measurements, the magnetic transition is only observable for $\mu_0 H$ = 0 T as a shoulder at $T_N(0)$ = 0.8 K (see also (*29*)).

The magnetic Bragg peak intensity in the quantum critical region

The temperature dependence of the position optimized peak intensity in the critical region between $\mu_0 H$ = 7 – 9.5 T is shown in fig. S2. Upon increasing magnetic field strength the magnetic intensity is gradually weakened and vanishes at $\mu_0 H^*$ ≈ 8 T for lowest temperatures in agreement with the field dependence shown in Fig. 2. For fields higher than 8 T the magnetic intensity increases providing evidence for a distinct magnetic phase.

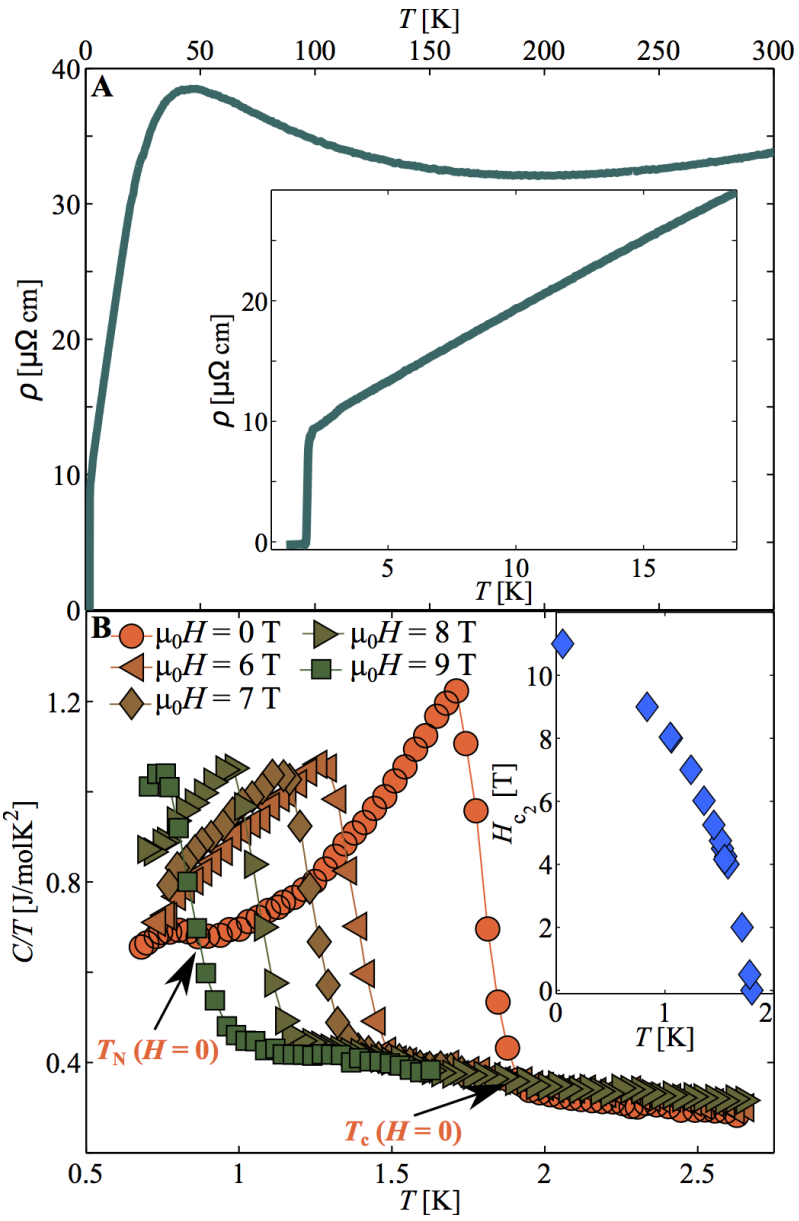

fig. S1. Macroscopic results. The electrical resistivity, measured along [1 0 0], as a function of temperature is shown in (**A**). The RRR equals 3.6. (**B**) displays heat capacity data for different magnetic fields applied in the basal plane. The inset reveals the upper critical field as a function of temperature measured via thermal heat capacity and electrical resistivity.

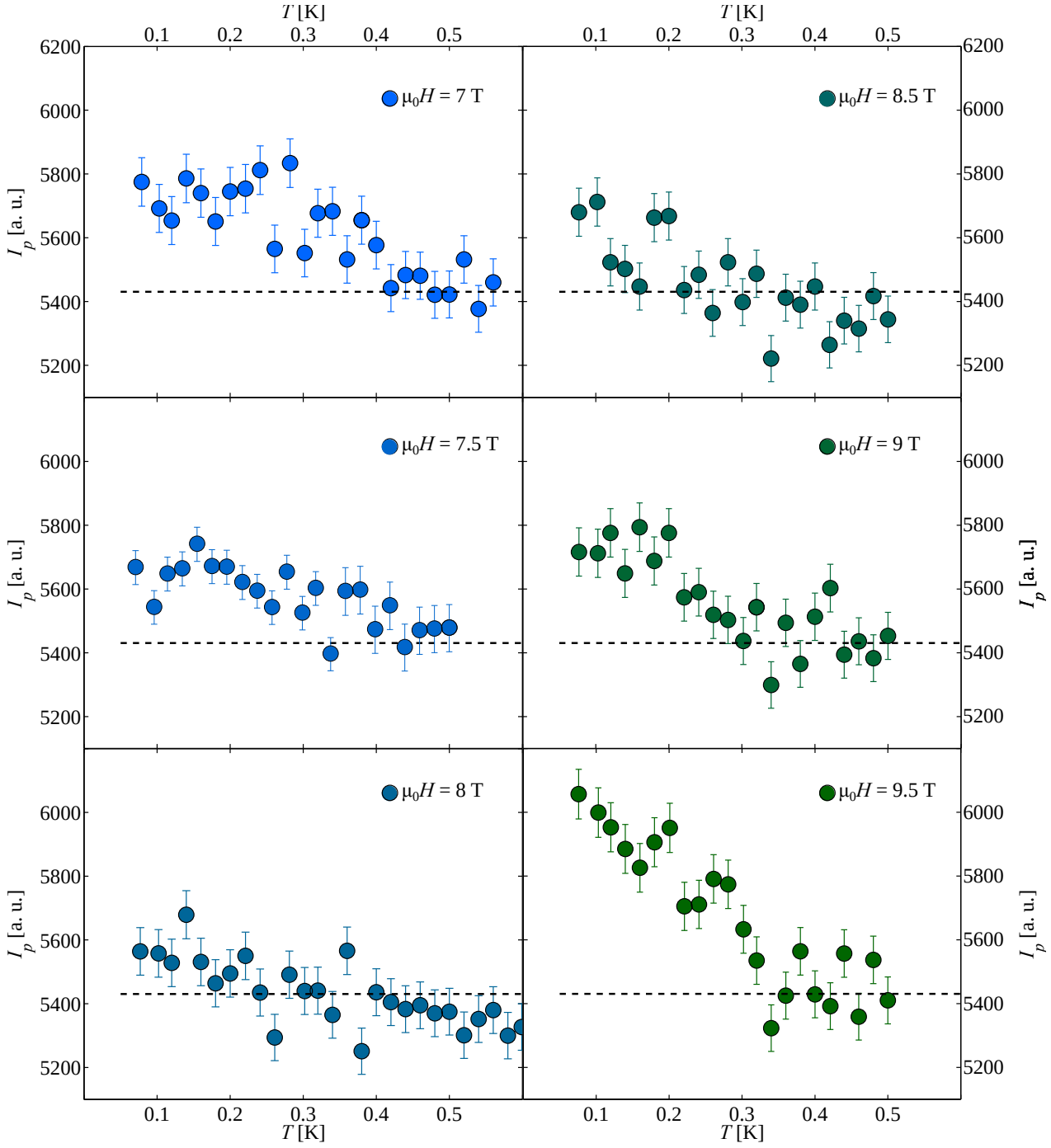

fig. S2. Temperature dependence of magnetic intensity in the critical region. The scan displays the temperature dependence of the position optimized peak intensity in the critical region around $\mu_0 H^* \approx 8$ T. The dashed line denotes the field-averaged background.